

Trapped Photoelectrons During Spacecraft Charging in Sunlight

Shu T. Lai, *Fellow, IEEE*, and Kerri Cahoy, *Member, IEEE*

Abstract—For a dielectric spacecraft charging in sunlight, the potentials are different on the sunlit and dark sides. Differential charging of spacecraft surfaces can trap low-energy electrons by means of potential wells and barriers. The low-energy electrons are mostly photoelectrons and secondary electrons. Motivated by the recent interest in trapped photoelectrons measured by the Van Allen Probes in the radiation belts, we calculate the extent of the trapped photoelectron area and the potential barrier as a function of the dipole strength and sun angle using the monopole-dipole model. We find that the dipole strength is an important parameter in controlling the behavior of the potential wells and barriers. The usual inequality, $1/2 \leq A \leq 1$ where A is the dipole strength, used in the monopole-dipole model can be relaxed and amended for finite sun angles. We then use a simple method to estimate the density of the trapped low-energy electrons in these areas. In sunlight charging, the low-energy electron population around the spacecraft is enhanced by the photoelectrons trapped inside the potential barrier.

Index Terms—Barrier, chorus waves, critical temperature, eclipse passage, electron density, electron temperature, geosynchronous environment, monopole-dipole potential, photoemission, potential well, radiation belts, saddle point, spacecraft charging, spacecraft charging in sunlight, trapped photoelectron, Van Allen Probes, wave-particle interaction.

I. INTRODUCTION

SPACECRAFT surface charging is due to excess electrons collecting on the surface [1], [2]. The ambient electron flux usually exceeds the ambient ion flux by about two orders of magnitude, because of the difference in electron and ion masses. The spacecraft voltage relative to the ambient plasma is governed by the current balance equation

$$\sum_k I_k = 0 \quad (1)$$

where k labels the various currents arriving at, or leaving from, the spacecraft surface. For example, (1) can be written as follows:

$$I_e(\phi) - I_s(\phi) - I_b(\phi) - I_i(\phi) - I_{ph}(\phi) = 0 \quad (2)$$

Manuscript received October 31, 2014; revised January 30, 2015 and June 15, 2015; accepted June 17, 2015. Date of publication August 7, 2015; date of current version September 9, 2015.

S. T. Lai is with the Space Propulsion Laboratory, Massachusetts Institute of Technology, Cambridge, MA 02137 USA, and also with the Institute for Scientific Research, Boston College, Newton, MA 02457 USA (e-mail: shlai11@mit.edu).

K. Cahoy is with the Space Telecommunications, Astronomy, and Radiation Laboratory, Massachusetts Institute of Technology, Cambridge, MA 02137 USA (e-mail: kcahoy@mit.edu).

Color versions of one or more of the figures in this paper are available online at <http://ieeexplore.ieee.org>.

Digital Object Identifier 10.1109/TPS.2015.2453370

where ϕ is the spacecraft potential. In (2), the subscripts e , s , b , i , and ph label the currents of the incoming ambient electrons, outgoing secondary electrons, outgoing backscattered electrons, incoming ambient ions, and outgoing photoelectrons, respectively.

Geometrical effects, surface properties, and anisotropy in currents can cause deviation from uniform charging. If there are more currents involved, they should be included in (2). For example, in ion beam propulsion, the beam currents emitted from the spacecraft should be added even if the beams are fully neutralized, because partial beam return may occur under certain conditions. Charged beam currents exceeding the ambient currents can artificially control the spacecraft potential. These are some complications outside the scope of this paper.

If the currents in (2) vary, the potential ϕ varies accordingly. Ambient electron and ion currents in space vary naturally, resulting in spacecraft potential variation. Recently, there has been interest in spacecraft potential fluctuations by chorus waves observed on the Van Allen Probe satellites [3], [4]. The spacecraft potential fluctuations have been attributed to the chorus wave-electron interaction affecting the photoelectron current of the spacecraft.

In this paper, we study trapped photoelectrons in the potential wells on the sunlit surfaces of spacecraft. If a spacecraft is conducting, the charging voltage in sunlight is usually a few volts (V) at the geosynchronous environment. As a result, a potential well of a few volts forms. The prominent solar ultraviolet line is ~ 10.2 eV, and the work function of the typical satellite surface materials is ~ 4 eV. Since the photoelectron flux at geosynchronous altitudes typically exceeds the ambient electrons flux by two orders of magnitude, the photoelectron current controls the spacecraft potential.

The potential wells can exist even when the spacecraft charges to high negative potentials in sunlight. A monopole-dipole potential, or even monopole-multipole potential, may form. Without the loss of generality, it is sufficient to use a monopole-dipole potential, which is simple, for demonstrating the trapping of photoelectrons. We calculate the density of the photoelectrons trapped, and obtain preliminary results.

II. MONOPOLE-DIPOLE POTENTIAL

For a satellite with nonconducting surfaces, the dark side can charge to high voltages, while the sunlit side charges to low voltages. The high voltage can extend to the sunlit side and block some photoelectrons emitted from the sunlit surface [5], [6]. This implies that charging to negative

potentials on the sunlit side is related to charging to the negative potentials on the dark side. If there is no charging on the dark side, the sunlit side does not charge to negative potentials. If charging on the dark side does not depend on the ambient electron density, then charging on the sunlit side does not depend on the ambient electron density either.

Let us study a simple monopole-dipole potential model

$$\phi(\theta, r) = K \left(\frac{1}{r} - \frac{A \cos \theta}{r^2} \right) \quad (3)$$

where $\theta = 0^\circ$ is the sun direction, K the monopole strength, A the normalized dipole strength, and r the radial distance from the satellite center. The potential barrier located at 0° is at R_S , where R_S is the distance from the satellite center

$$\left[\frac{d\phi(\theta=0, r)}{dr} \right]_{r=R_S} = 0 \quad (4)$$

which gives

$$R_S = 2A \cos \theta. \quad (5)$$

Let us denote R as the satellite radius. Since R_S must be outside the spacecraft, the location of the barrier R_S must be greater than R . Therefore, (5) implies the inequality

$$2A \cos \theta > R. \quad (6)$$

The validity of the dipole approximation requires that the second term in (3) is less than the first term. Therefore, inequality (6) becomes

$$R > A \cos \theta > R/2. \quad (7)$$

The potential barrier height B is given by

$$B = \phi(\theta, R_S) - \phi(\theta, R) = K \frac{(2A \cos \theta - R)^2}{4A \cos \theta R^2}. \quad (8)$$

Photoelectrons and secondary electrons have a few electron volts in energy. The barrier height B can be small (a few volts) to block the photoelectrons and secondary electrons, i.e., $(R - 2A \cos \theta)$ can be small.

In Fig. 1, the spacecraft radius is $R = 1$. The potential profiles at $\theta = 0^\circ$ or 180° are shown for $A = 0.5, 0.7, 0.9, 1.1$, and 1.3 . For A less than 0.5 , there is no potential well, and therefore the photoelectrons are completely repelled. In Fig. 2, the potential profiles at $\theta = 48^\circ$ are shown for $A = 0.5, 0.75, 1.0, 1.25$, and 1.5 . For $A = 0.75$ or less, the barrier height B is zero, and therefore there is no potential well. Without a potential well, the photoelectrons are repelled, and they escape completely.

One can plot the loci of the barrier for various values of θ on the sunlit side. The results (Fig. 3) look like polar caps. Low-energy electrons of a few electron volts are trapped in the potential wells. Since photoelectrons and secondary electrons are of low energy, they can be trapped by the potential barriers.

Since photoelectrons are much more abundant than the secondary electrons, the electrons in the potentials are mostly photoelectrons. As a result, the trapped photoelectrons enhance the electron density in the polar cap region.

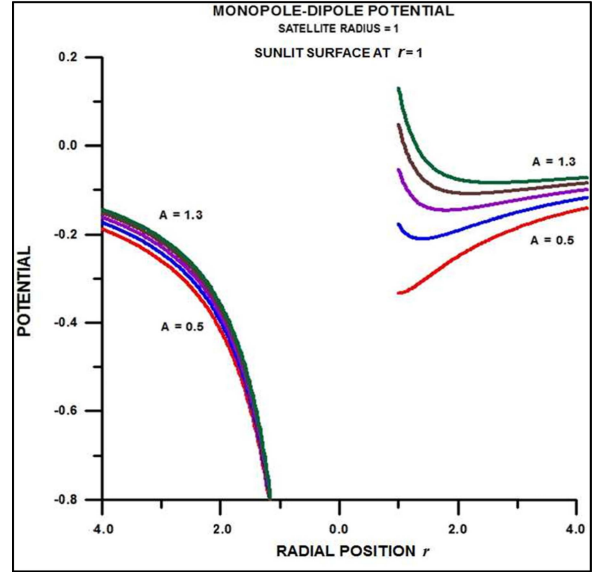


Fig. 1. Example of potential profiles on the sunlit ($\theta = 0^\circ$) and dark sides ($\theta = \pi$) in a monopole-dipole model (3). The surfaces are at $r = 1$. The sun is on the right-hand side. The monopole strength $K = -1$. The potentials are normalized by the magnitude of the potential at $r = 1$ and $\theta = \pi$. Note that a potential barrier (a dip) forms on the sunlit side when $A > 0.5$. For $\theta = 0^\circ$, the monopole-dipole model requires $1 > A > 0.5$ to satisfy inequality (7).

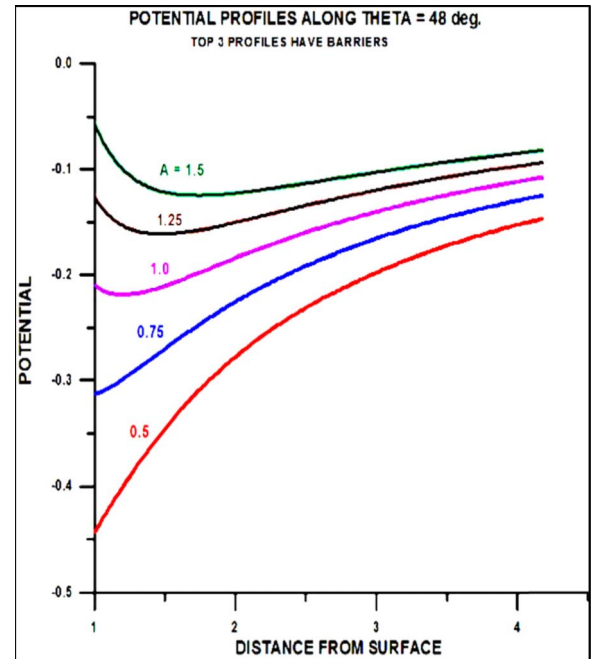


Fig. 2. Potential profiles along the radial distance at $\theta = 48^\circ$ are shown. The satellite radius $R = 1$. The monopole strength $K = -1$. The potentials are normalized by the magnitude of the potential at $r = 1, \theta = \pi$. Note that the top three profiles have potential barriers (dips), but the lower ones have not. A needs to be $>(R/2)/\cos(48^\circ)$ to satisfy inequality (7).

Suppose the trapped electrons form a velocity distribution. One can calculate the fraction L of the total electron flux escape over the barrier B

$$L = \frac{\int_B^\infty dEE f(E)}{\int_0^\infty dEE f(E)} \quad (9)$$

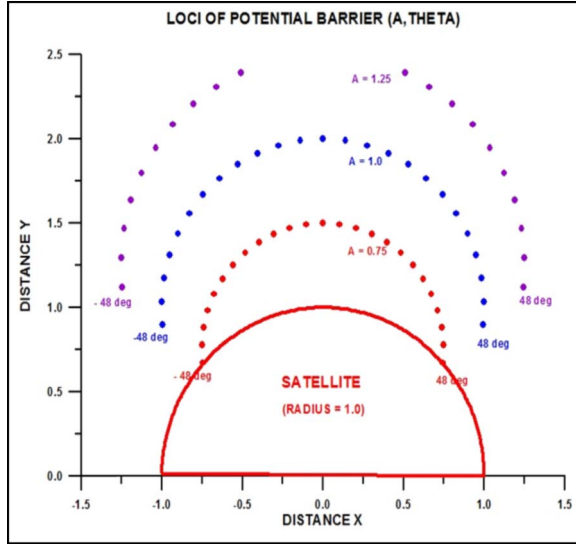


Fig. 3. Loci of potential barrier as a function of A and θ on the sunlit side. The sun at $\theta = 0^\circ$ is vertically above. The loci delineate potential well regions like polar caps.

where we have used $E = (1/2)mv^2$. For an approximation, let the photoelectron velocity distribution be Maxwellian [7], and one obtains an analytical result of L as follows:

$$L = \frac{\int_B^\infty dE E \exp(-E/kT)}{\int_0^\infty dE E \exp(-E/kT)} = \left(\frac{B}{kT} + 1 \right) \exp\left(-\frac{B}{kT}\right). \quad (10)$$

From (10), one can easily plot the fraction L as a function of the barrier height B divided by the photoelectron temperature kT . If some external force perturbs the electron energy, the fraction L varies accordingly.

III. ELECTRON DENSITY

The velocity integral of the Maxwellian electron velocity distribution $f(v)$ gives the electron density n in a 3-D space without blockage. Suppose that the electrons are blocked and the measurements are made on a surface, or sensor, facing the barrier. The electrons more energetic than the barrier energy escape, but those with less energy return and have density n_B . The velocity integral is of the form

$$n_B = \int_0^{v_B} dv v^2 \int_0^\pi d\phi \int_0^{2\pi} d\theta \sin \varphi f(v) \quad (11)$$

where v_B is the velocity given by $(1/2)mv_B^2 = B$. The Maxwellian distribution $f(v)$ is as follows:

$$f(v) = n \left(\frac{m}{2\pi kT} \right)^{3/2} \exp\left(-\frac{mv^2}{2kT}\right). \quad (12)$$

Let us use the variables x , where $x = (mv^2/2kT)^{1/2}$ and $W = (B/kT)^{1/2}$. Equation (11) becomes

$$n_B = \frac{2\pi n}{\pi^{3/2}} \int_0^W dx x^2 \exp(-x^2). \quad (13)$$

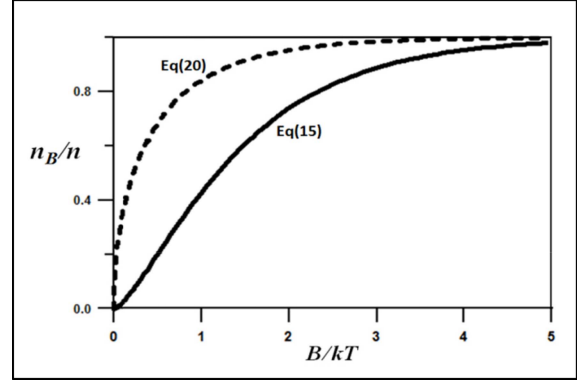


Fig. 4. Normalized trapped photoelectron density n_B/n plotted as a function of normalized barrier height B/kT . As the barrier height B/kT increases, the ratio n_B/n approaches unity asymptotically.

Integrating by parts, (13) becomes

$$n_B = \frac{2\pi n}{\pi^{3/2}} \left[\int_0^W dx \exp(-x^2) - [x \exp(-x^2)]_0^W \right] \quad (14)$$

$$\frac{n_B}{n} = \left[\text{erf}(W) - \frac{2}{\pi^{1/2}} W \exp(-W^2) \right] \quad (15)$$

where the error function $\text{erf}(W)$ is given by

$$\text{erf}(W) = \frac{2}{\sqrt{\pi}} \int_0^W dx \exp(-x^2). \quad (16)$$

Fig. 4 shows a plot of n_B/n as a function B/kT . The photoelectron flux measured is $\sim 2 \times 10^{-9} \text{ A cm}^{-2}$ for typical satellite surface materials [8]. Taking a photoelectron temperature of $\sim 1.5 \text{ eV}$, one obtains the photoelectron density $n \approx 3 \times 10^2 \text{ cm}^{-3}$. Substituting this value of n into (13), one obtains the density n_B of blocked electrons as a function of barrier potential B . For example, let the barrier height B be 1 eV and the photoelectron temperature be 1.5 eV, then the ratio n_B/n is ~ 0.3 in the equilibrium model and ~ 0.78 in the 1-D model, which is discussed in Section IV. For $n \approx 300 \text{ cm}^{-3}$, this graph gives $n_B \approx 100 \text{ cm}^{-3}$ and 234 cm^{-3} , respectively. This method offers an estimate of the trapped photoelectron density n_B .

IV. 1-D MODEL

In the trapped region, the electrons bounce about at equilibrium. They can escape through the lowest potential B at the saddle point of the barrier as discussed above.

Alternatively, one may argue for a 1-D model in which the velocity of an electron emitted at an angle φ has to exceed $v_B/\cos\varphi$ in the radial direction. The velocity v_B is the velocity related to the barrier potential, that is, its energy has to exceed $B/\cos^2\varphi$. The flux ratio L in (9) becomes

$$L = \frac{\int_0^{2\pi} d\theta \int_0^{\pi/2} d\varphi \sin \varphi \int_0^{v_B/\cos\varphi} dv v^2 \cos \varphi}{\int_0^{2\pi} d\theta \int_0^{\pi/2} d\varphi \sin \varphi \int_0^\infty dv v^2 \cos \varphi}. \quad (17)$$

Converting the velocity variable v into energy E and canceling the angles as usual, (17) becomes

$$L = \int_0^1 dy (B/kTy + 1) \exp(-B/kTy) \quad (18)$$

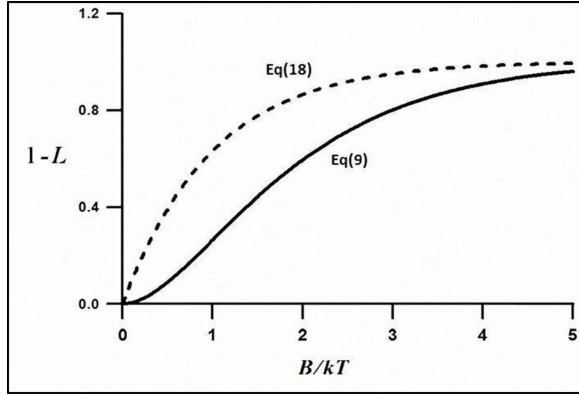


Fig. 5. Fractions of the trapped electrons as a function of the normalized potential barrier. As the barrier height increases, $1 - L$ approaches unity asymptotically, where all the electrons are trapped and $n_B/n = 1$.

where $y = \cos^2 \phi$. The fractions of trapped electrons as given in (9) and (18) are shown in Fig. 5. It is more difficult for the electrons to escape in the $v_B/\cos\phi$ model. Therefore, there are more trapped electrons.

With the energy term $B/\cos^2\phi$, the trapped electron density, (15), becomes

$$n_B = \int_0^{V_B/\cos\phi} dv v^2 \int_0^\pi d\phi \int_0^{2\pi} d\theta \sin\phi f(v). \quad (19)$$

Integrating over v and θ , one obtains

$$\frac{n_B}{n} = \int_0^\pi d\phi \sin\phi [\text{erf}(W') - \frac{2}{\pi^{1/2}} W' \exp(-W'^2)] \quad (20)$$

where $W' = (B'/kT)^{1/2}$ and $B' = B/\cos^2\phi$.

The result in (20) is added as a dashed line in Fig. 4. With the barrier energy $B/\cos^2\phi$, the trapping is more efficient. As the barrier height increases, the trapping increases. Eventually, as the trapping approaches unity, the trapped electron density approaches that of the density of the low-energy electrons (photoelectrons and secondary electrons) emitted from the surface.

V. GENERAL COMMENTS

We have neglected secondary electrons because the photoelectron flux from satellite surfaces usually exceeds the ambient electron flux by an order of magnitude or more. One can include the secondary electrons, but the conclusion would be about the same.

An interesting question is whether a self-consistent solution of photoelectron flux trapped in the dipole potential well can be formulated. We believe that the answer is yes. The fraction of photoelectrons trapped is a function of the photoelectron energy spectrum and the potential difference between the barrier and the sunlit surface. The surface potential, in turn, is given by the current balance between the fluxes of the ambient electrons, incoming ions, escaping photoelectrons, and secondary electrons. The potential difference between the sunlit surface and the dark surface determines the dipole strength

$$\frac{A}{R} = \frac{\phi(180^\circ, R) - \phi(0^\circ, R)}{\phi(180^\circ, R) + \phi(0^\circ, R)}. \quad (21)$$

For a typical example, if $\phi(180^\circ, 1) = -1000$ V and $\phi(0^\circ, 1) = -5$ V, (21) gives $A/R \approx 0.99$. The dipole strength, in turn, controls the barrier (8). We believe that such a self-consistent scheme would be an interesting project for future research work.

The solar energy spectrum varies in a solar cycle. It affects the photoelectron energy distribution and flux from the sunlit surfaces. It would be interesting if the onboard instruments available are accurate enough to measure the trapped photoelectron variation over a solar cycle. The instrument should have the capability for measuring the energy distribution of the trapped photoelectrons and secondary electrons on the sunlit side. The maximum energy of the trapped electrons indicates the barrier height.

For a figure of supporting data, we refer to [10, Fig. 3]. The figure shows the observed evidence of low-energy electrons (photoelectrons and secondary electrons) trapped by local potentials on the surfaces of Los Alamos Laboratory Satellite 1994-084 in sunlight [11] (courtesy of M. F. Thomsen). In [10, Fig. 3], the barrier height is ~ 10 eV from 17.9 to 21 UT.

VI. CONCLUSION

This paper stresses the importance of differential charging of spacecraft in sunlight. The dark side can charge to high negative potentials, while the sunlit side to low potentials. The monopole-dipole model can be used to reveal that there can exist potential wells and barriers. The barrier can trap low-energy electrons such as photoelectrons. The fraction of the escaping electron cloud can be calculated. The fraction varies if the barrier height or the electron temperature varies.

In sunlight charging, the low-energy electron population around the spacecraft is enhanced by the photoelectrons trapped inside the potential barrier. If the photoelectrons are trapped, the sunlit side does not charge to a positive potential.

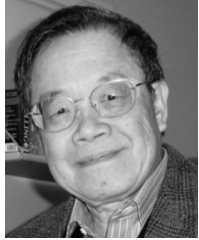
ACKNOWLEDGMENT

The authors would like to thank M. F. Thomsen for the helpful discussion and A. G. Rubin for reading the manuscript. They would also like to thank the referees for enlightening and stimulating remarks. S. T. Lai would like to thank M. Martinez-Sanchez of MIT and C. P. Pike of BC for hospitality.

REFERENCES

- [1] D. Hastings and H. Garrett, *Spacecraft-Environment Interactions*. Cambridge, U.K.: Cambridge Univ. Press, 1996.
- [2] S. T. Lai, *Fundamentals of Spacecraft Charging—Spacecraft Interactions With Space Plasmas*. Princeton, NJ, USA: Princeton Univ. Press, 2011.
- [3] D. M. Malaspina *et al.*, “Chorus waves and spacecraft potential fluctuations: Evidence for wave-enhanced photoelectron escape,” *Geophys. Res. Lett.*, vol. 41, no. 2, pp. 236–243, Jan. 2014.
- [4] X. Wang, D. M. Malaspina, R. E. Ergun, and M. Horányi, “Photoelectron-mediated spacecraft potential fluctuations,” *J. Geophys. Res.*, vol. 119, no. 2, pp. 1094–1101, Feb. 2014.
- [5] A. L. Besse and A. G. Rubin, “A simple analysis of spacecraft charging involving blocked photoelectron currents,” *J. Geophys. Res.*, vol. 85, no. A5, pp. 2324–2328, May 1980.
- [6] S. T. Lai and M. F. Tautz, “Aspects of spacecraft charging in sunlight,” *IEEE Trans. Plasma Sci.*, vol. 34, no. 5, pp. 2053–2061, Oct. 2006.
- [7] E. C. Whipple, “Potentials of surfaces in space,” *Rep. Prog. Phys.*, vol. 44, no. 11, p. 1197, 1981.

- [8] B. Feuerbacher and B. Fitton, "Experimental investigation of photoemission from satellite surface materials," *J. Appl. Phys.*, vol. 43, no. 4, pp. 1563–1572, 1972.
- [9] C. K. Purvis, H. B. Garrett, A. C. Whittlesey, and N. J. Stevens, "Design guidelines for assessing and controlling spacecraft charging effects," NASA, Washington, DC, USA, Tech. Rep. 2361, Sep. 1984.
- [10] S. T. Lai, "Some novel ideas of spacecraft charging mitigation," *IEEE Trans. Plasma Sci.*, vol. 40, no. 2, pp. 402–409, Feb. 2012.
- [11] M. F. Thomsen, H. Korth, and R. C. Elphic, "Upper cutoff energy of the electron plasma sheet as a measure of magnetospheric convection strength," *J. Geophys. Res., Space Phys.*, vol. 107, no. A10, p. 1331, Oct. 2002.



Shu T. Lai (M'80–SM'88–F'05) received the Ph.D. degree in physics from Brandeis University, Waltham, MA, USA, in 1971, and the Certificate of Special Studies in administration and management from Harvard University, Cambridge, MA, USA, in 1986.

He has authored many papers and two books entitled *Fundamentals of Spacecraft Charging* by Lai, S.T., (Princeton, NJ, USA: Princeton University Press, 2011) and *Spacecraft Charging* by Lai, S.T. (editor), (Reston, VA, USA: AIAA Press, 2011).

Dr. Lai is a fellow of the Institute of Physics and the Royal Astronomical Society, and an Associate Fellow of the American Institute of Aeronautics and Astronautics (AIAA). He was the Chair of the AIAA Atmospheric and Space Environments Technical Committee from 2003 to 2005. He is a Senior Editor of the IEEE TRANSACTIONS ON PLASMA SCIENCE.



Kerri Cahoy (M'12) received the B.S. degree in electrical engineering from Cornell University, Ithaca, NY, USA, in 2000, and the M.S. and Ph.D. degrees in electrical engineering from Stanford University, Stanford, CA, USA, in 2002 and 2008, respectively.

She was a Senior Payload Engineer with Space Systems Loral. She was a NASA Post-Doctoral Program Fellow with the NASA Ames Research Center, Mountain View, CA, USA, and a Research Scientist with the MIT/NASA Goddard Space Flight Center. She is currently a Boeing Assistant Professor with the Department of Aeronautics and Astronautics, Massachusetts Institute of Technology, Cambridge, MA, USA.